

## Section 1: Simulating Wigner rotation as a Unitary gate

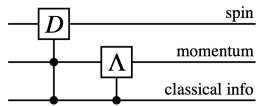


FIG. 1: Relativistic state transformation as a quantum circuit: the gate  $D$  which represents the matrix  $D_{\text{cr}}[W(A, p)]$  is controlled by both the classical information and the momentum  $p$ , which is itself subject to the classical information  $A$ .

This section is inspired by foundational paper on relativistic quantum information and tries to simulate the below circuit from the paper:



The circuit represents spin state transformation based on momentum and classical information. Our aim here is to model this circuit into quantum simulation using qiskit and model the Wigner rotation acting as a single qubit unitary operator on the spin degree of freedom.

In the simulation, we consider a spin-1/2 particle whose momentum is known and we observe how spin state is transformed for observers under different inertial frames with Lorentz boost fixed in z-direction. Six different momentum directions are considered and velocities range from 0.01-0.99. We calculate wigner rotation for all momentum-velocity combinations as below:

$$\theta = 2 \cdot \arctan \left( \frac{\sinh(\eta) \cdot \sin(\alpha)}{\cosh(\eta) + \sinh(\eta) \cdot \cos(\alpha)} \right),$$

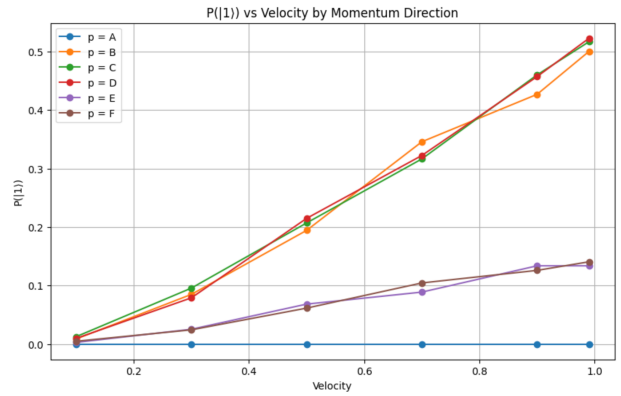
where  $\eta$  is the rapidity derived from the velocity ( $\eta = \text{arctanh}(v)$ ), and  $\alpha$  is the angle between the boost vector and the momentum vector.

The axis of rotation is given by cross product of boost direction and momentum. The axis is used to make a hermitian operator as combination of Pauli matrices and hence creating the unitary operator  $U = \exp(-i \cdot \theta/2 \cdot G)$ . Where  $G = n_x \sigma_x + n_y \sigma_y + n_z \sigma_z$ . This encodes SU(2) transformation of the spin qubit under a Lorentz boost based on momentum.

A simple circuit as below is simulated in qiskit (QCMDL\_project) file:

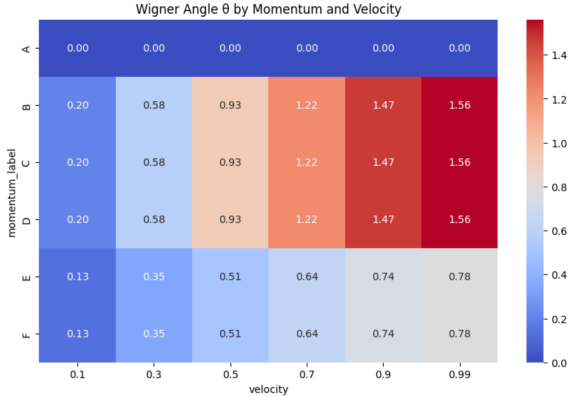
### Output

1. P(1) vs Velocity by Momentum Direction: The plot shows how

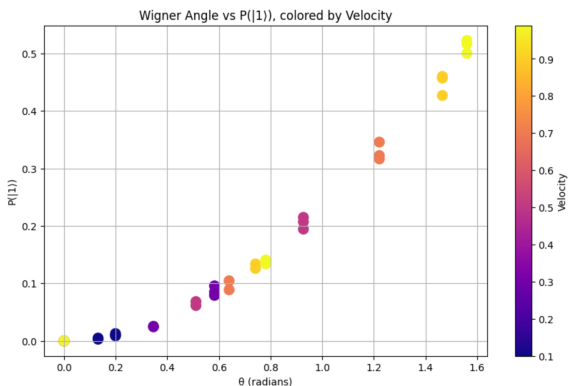


probability of measuring the spin in  $|1\rangle$  state changes with velocity for different momentum directions labeled A-F. Momentum B, C & D which have significant components orthogonal to the boost direction, the probability of measuring  $|1\rangle$  increases and at  $v=0.99$  is almost greater than 0.5. They have a larger Wigner rotation. Momentum A is parallel to boost, hence no rotation and spin state remains in  $|0\rangle$  state. E & F have some components parallel to the boost hence less rotation.

2. This is exact quantitative result for point 1. Momentum A corresponds to 0 rotation for all V. B, C & D have increasing Wigner angle with velocity. E & F, due to partial alignment with boost have less rotation.



3. In plot Wigner angle vs  $P(|1\rangle)$ , the main observation to note is that for different values of velocity, there's a cluster and similar Wigner angle. This shows that velocity is not the only factor in determining spin measurement outcome.

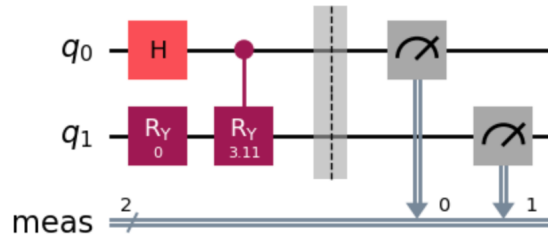


## Section 2: Spin-Momentum Entanglement via Controlled Wigner Rotation

This section is based on the paper “Spin-momentum correlation in relativistic single particle quantum states” by M. A. Jafarizadeh & M. Mahdian. The paper shows how the spin of a single particle entangles with its momentum under a Lorentz boost. The spin state transformation is no longer independent but depends on controlled unitary spin rotation based on momentum. The spin qubit undergoes a Wigner rotation only when momentum qubit is in a specific eigenstate.

Though not explicitly given in the paper, we construct a circuit consisting of 2 qubits in  $|0\rangle$  state representing momentum degree of freedom and spin. Here we

consider superposition of 2 momentum eigenstates  $|p_1\rangle$  &  $|p_2\rangle$  (perpendicular to Lorentz boost), where  $|p_2\rangle$  is associated with momentum basis state  $|1\rangle$  and only  $|p_2\rangle$  undergoes a Wigner rotation due to Lorentz boost.



We apply hadamard on the momentum qubit, putting it in superposition state of  $|0\rangle + |1\rangle/\sqrt{2}$  tensor  $|0\rangle$ . The spin qubit undergoes:

1. A base rotation of  $Ry(\omega_1)$
2. A controlled rotation  $Ry(\omega_2 - \omega_1)$  with momentum qubit as controlled. This is an additional rotation when momentum is  $|1\rangle$
3. Omega2 is declared as  $\pi^*v$  and for simplicity this Wigner angle is considered proportional to velocity ( $\Omega_2 = \pi^*v$ ) unlike in section 1 where we calculated Wigner angle using momentum and rapidity

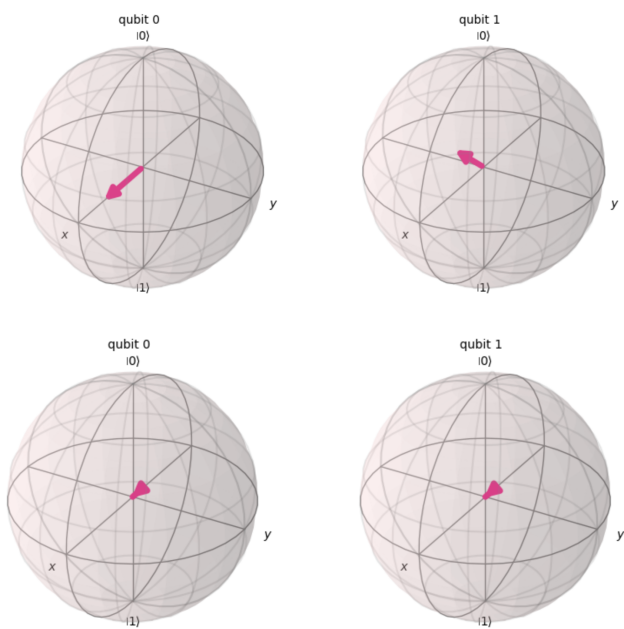
As mentioned in the spin-momentum entanglement paper, for special scenario of  $\omega_1 \rightarrow 0$  and  $\omega_2=\pi$ , this controlled gate acts like a CNOT gate. We will see this mathematically and then visualise on bloch sphere.

State after hadamard on first qubit -  $|\Psi\rangle = |0\rangle_s \otimes (|0\rangle_p + |1\rangle_p)/\sqrt{2}$   
 the base rotation and controlled rotation can be expressed as matrix shown in paper:  $U = |0\rangle\langle 0|_p \otimes R(\omega_1) + |1\rangle\langle 1|_p \otimes R(\omega_2)$ .  $R(w)$  is the unitary rotation around y axis. Applying this to the state and considering  $\omega_1 = 0$  and  $\omega_2 = \pi$  to see CNOT behaviour. At  $\omega_1=0$ ,  $R(\omega_1)$  becomes Identity and state becomes  $|\Psi'\rangle = (|0\rangle_s \otimes |0\rangle_p + R(\omega_2)|0\rangle_s \otimes |1\rangle_p)/\sqrt{2}$ . When  $\omega_2=\pi$ ,  $|\Psi'\rangle = (|0\rangle \otimes |0\rangle - |1\rangle \otimes$

$|11\rangle/\sqrt{2}$ , a bell state and we can see that the spin qubit is flipped.

Then, to study the spin momentum entanglement, the partial trace is taken over momentum qubit to get the reduced density matrix for spin system

A simple circuit is simulated in qiskit (QML\_project) file:



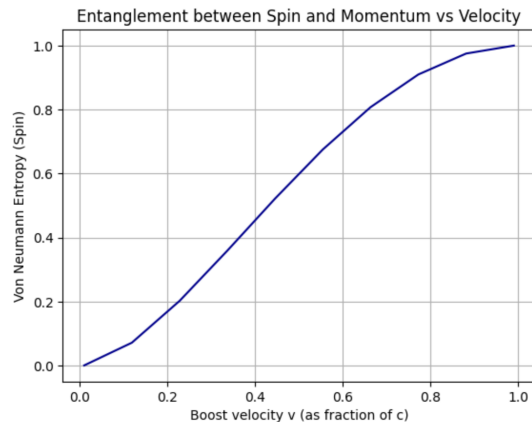
### Output:

With left bloch sphere for momentum qubit and right for spin. We see that at lower velocity where omega 2  $\rightarrow 0$  (because  $\omega_2 = \pi v$ ), we have no rotation. As the velocity increases, the spin and momentum starts getting entangled when  $v=0.5$ , the spin and momentum starts getting entangled as shown in figure.

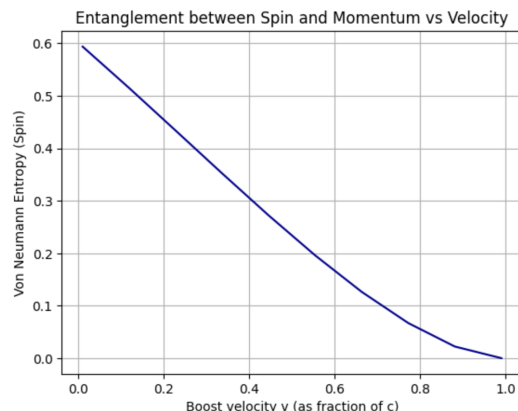
At  $v=1$ , maximum entanglement is reached as shown in figure2. And above we calculated the bell state  $(|00\rangle - |11\rangle)/\sqrt{2}$

Entropy vs velocity (for different values of Wigner angles):

1. Omega1 = 0 and omega2 =  $\pi v$ , we saw above that at  $v \sim 1$ , maximum entanglement is reached. The plot of entropy vs velocity confirms this.

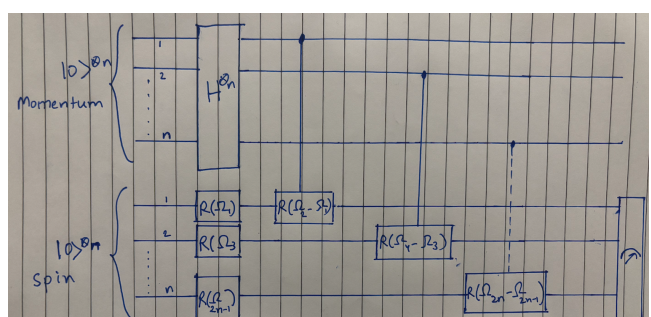


2. For  $\Omega_1 = \pi/2$  and  $\Omega_2 = \pi/2$ . There is base rotation of  $R_y(\pi/2)$ , putting the spin qubit in  $|+\rangle$  state. The controlled rotation  $R_y(\Omega_2 - \Omega_1) = R_y(-\pi/2)$  for  $v > 0$ , undo the rotation. Hence, the state becomes  $1/\sqrt{2}(|0\rangle + |+\rangle + |1\rangle)$ . This is a non separable state. That is why at  $v=0$ , entropy is non zero. As the velocity increases and gets close to 1. The controlled rotation becomes  $R_y(0)$ , no



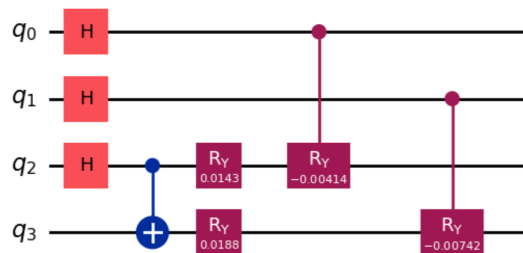
rotation and we get a pure separable state.

3. This circuit can be further extended to multiple qubits with their respective spin and momentum qubits and Wigner angles. Below is a circuit diagram for the same.



### Section 3: Quantum Entanglement of moving bodies

Building upon the previous section and taking inspiration from paper “Quantum Entanglement of moving bodies” by Gingrich and Adani. In previous section, we had 1 particle system and 2 qubits representing their momentum degree of freedom and spin. Here we take 2 particle system. 2 qubits representing momentum degree of freedom and 2 qubits representing their respective spin. We explore how relativistic transformations impact spin-spin entanglement initially prepared in bell state.



The circuit consists of:

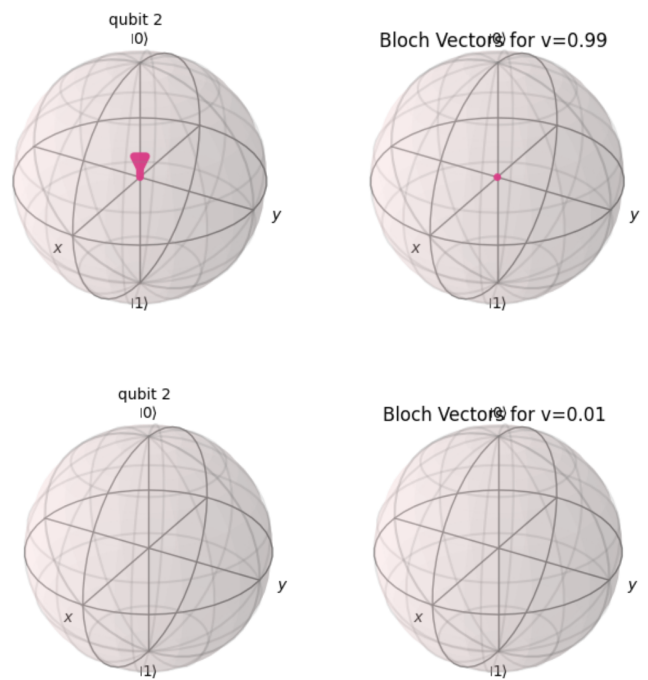
1. 2 qubits q0 and q1 representing discrete momentum eigenstates of particle A and B, initially prepared in superposition by applying hadamard simulating multiple possible eigenstates. We specifically define 4 momentum vectors such as [0,1,0,], [1,0,0] and such to see effect of velocity along with different momentum directions.
2. 2 spin qubits q2 and q3 are prepared in bell state, representing maximal spin-spin entanglement
3. Wigner rotations are then applied based on formula used in section 1. A base rotation is applied on both qubits based on Wigner angles for p1 and p3 and a controlled rotation is applied for angles delta\_A and delta\_B defined as  $\text{delta\_A} = \text{wigner\_angles['p2']} - \text{wigner\_angles['p1']}$  &  $\text{delta\_B} =$

$\text{wigner\_angles['p4']} - \text{wigner\_angles['p3']}$

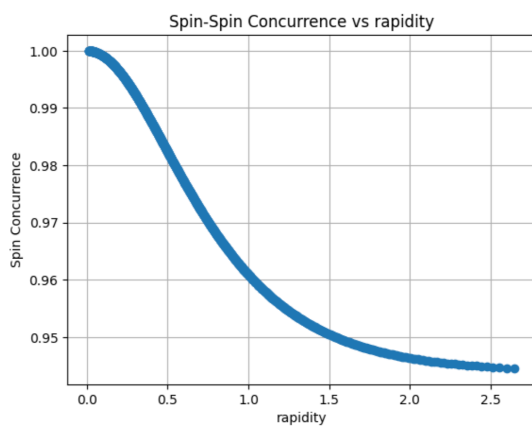
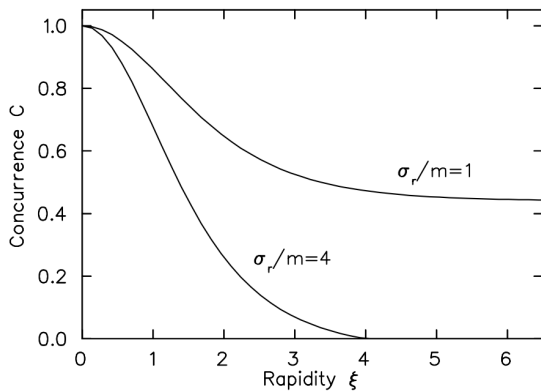
4. We run the circuit for different values of velocities ranging from 0.01 -099.

Output:

1. We analyse the bloch sphere for spin qubits which are initially maximally entangled. The momentum qubits are always in  $|+\rangle$  state pointing towards x-axis. The spin qubits for chosen momentum vectors do not undergo any change within lower range of velocities. At higher ranges the state starts losing it's entanglement. Below are bloch spheres of spin qubits at  $v= 0.01$  and  $v=0.99$ .

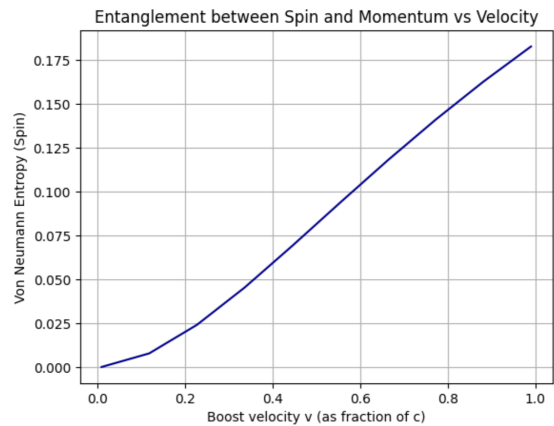


2. Now we compare the concurrence which is the measure of spin-spin entanglement achieved from our circuit and what is given in the reference paper by Gingrich and Adani, where increase in rapidity redistributes entanglement from spin-spin to spin-momentum. The figure on the left from the reference paper shows



concurrence vs rapidity for 2 distinct momentum distributions with narrow and wide momentum distributions for  $\sigma_r/m = 1$  &  $\sigma_r/m = 4$  respectively. Our simulation graph on the right is similar in lines of concurrence being 1 at near zero velocities confirming maximal entanglement. As velocity increases entanglement decreases. However, the magnitude of reduction in our simulation suggests case closed to narrow momentum somewhat closer to  $\sigma_r/m = 1$ . We initialised our momentum state as superposition of discrete eigenstates whereas in the paper it is depicted as continuous gaussian wave packets.

3. Just as we did in section 2, we now plot entropy vs velocity to see the spin-momentum entanglement. This highlights the transfer of entanglement from spin-spin to spin-momentum
4. To further support our case, let's examine the initial and final reduced



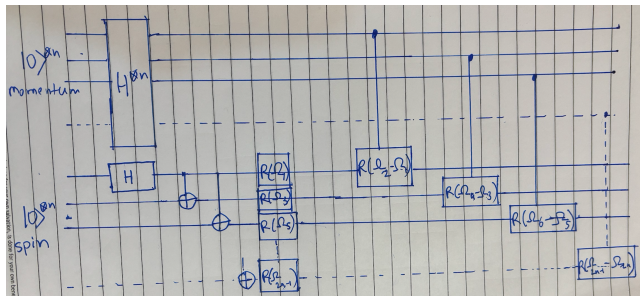
spin state by tracing over momentum. Initially at  $v=0.01$ , we have almost perfect entanglement, whereas the right matrix shows that at higher velocities entanglement decreases.

$$\rho = \begin{bmatrix} 0.499996757 & -0.000702819 & 0.000702819 & 0.499996757 \\ -0.000702819 & 0.000003243 & -0.000003243 & -0.000702819 \\ 0.000702819 & -0.000003243 & 0.000003243 & 0.000702819 \\ 0.499996757 & -0.000702819 & 0.000702819 & 0.499996757 \end{bmatrix}$$

$$\rho = \begin{bmatrix} 0.47905 & -0.05741 & 0.05741 & 0.47905 \\ -0.05741 & 0.02095 & -0.02095 & -0.05741 \\ 0.05741 & -0.02095 & 0.02095 & 0.05741 \\ 0.47905 & -0.05741 & 0.05741 & 0.47905 \end{bmatrix}$$

5. By playing with the momentum vectors, we can explore and understand more. An example, for a different momentum values, (intentionally leaving output graphs here) we will find that the graph of entropy vs velocity varies such that starting at value greater than zero at velocity equal to zero. The entropy first drops and then increases with velocity. Hence, this proves our analysis in section 1 that velocity is not the only factor in determining spin measurement outcomes under a relativistic setting.

This circuit can be extended to n qubits as per the below circuit:



## Future Work

We lay a foundation for exploring relativistic quantum information using quantum circuits with above simulations. As next steps, we will study the above phenomenon in detail by:

1. Simulating momentum as a gaussian wave packet instead of superposition of momentum eigenstates. This will help in understand relation between spin-spin and spin-momentum entanglement better.
2. Explore communication under relativistic settings: Simulate quantum teleportation where entangled particles undergo Wigner rotation. For a more realistic setting, we can add classical gates for delay to study how classical relativity also affects the setup and communication.
3. Use variation algorithms such as VQE to optimise Wigner angles to preserve entanglement under a relativistic transformation. We will try to define a cost function to study deviation from a target entangled state and use classical optimisers to adjust the Wigner angles.